NAOJ-ALMA-ENG-0007-A
2024-10-22

ALMA Memo 629

Quantization correction for auto and cross power spectra in the spectral domain

Kamazaki, T. [*1], and Kameno, S.
ALMA project office, National Astronomical Observatory of Japan,
2-21-1 Osawa Mitaka Tokyo 181-8588, Japan
[*1] *kamazaki.takeshi@nao.ac.jp*
2024-10-22

Abstract

In radio astronomical observations, astronomical signals can be regarded as Gaussian distributed noise with limited bandwidth and as a stationary process within a certain time range. To compensate for quantization distortion of the auto and cross power spectra obtained from such signals, we have prepared quantization correction in the spectral domain. The correction uses linear relation, which can be derived from assuming low correlation coefficients, between spectra with and without quantization. Thus, different from conventional methods in the lag domain (e.g., the Van Vleck correction), the prepared correction can be directly applied to auto and cross power spectra. The assumption is valid in many of radio astronomical observations, and hence the correction is usually applicable to them. In this memo, we focus on 3-bit digitizers that are used in Atacama Large Millimeter/submillimeter Array, derive their linear relation, and verify the correction using the relation in computational simulation.

1. Signal distortion by 3-bit quantization

Atacama Compact Array (ACA) in Atacama Large Millimeter/submillimeter Array (ALMA) is composed of Total-Power (TP) and 7-m arrays, which are responsible for taking total power and short baseline data for high fidelity imaging in ALMA. ACA Correlator [1] was originally dedicated to the calculation of auto and cross power spectra of digitized receiver signals from the two arrays. In Cycle 10, ACA Spectrometer is officially deployed and starts to process data from the TP array, and ACA Correlator is used for the 7-m array only. For the digitization of analog receiver signals, ALMA adopts 3-bit 4Gsps digitizers [2,3], whose input-output relation is shown in Figure 1, and transmitted to three digital backends (ALMA Correlator [4], ACA Correlator, and ACA Spectrometer) in digital format for further processing. The 3-bit digitizers affect the signals by quantization noise, which can be seen as nonlinear power responses in auto-power spectra (see Figure 2) and reduced correlation coefficients, which also show nonlinear response especially at

higher correlation coefficients, in cross-power spectra (see Figure 3). The distortion needs to be compensated, especially for total-power observations and system temperature measurements with the ACA Correlator. Thus, we initially prepared quantization correction in the spectral domain to compensate for the nonlinearity of auto-power spectra, and then this is expanded for cross-power spectra of future correlators and spectrometers in ALMA.

This memo describes the correction in the spectral domain to compensate for the distortion by the ALMA 3-bit digitizers, which is hereafter referred to as "auto-correlation correction" in auto-power spectra and "cross-correlation correction" in cross-power spectra. First, we list symbols and definitions common to the two corrections in Section 2. Second, we describe the auto-correlation correction in the spectral domain for auto-power spectra in Section 3 and the cross-correlation correction in the spectral domain for cross-power spectra in Section 4. Finally, computational simulation results are presented to confirm the corrections in Section 5. Since the auto-correlation correction is already used in the post-processing of the ACA Correlator, its parameters are summarized in Appendix D.

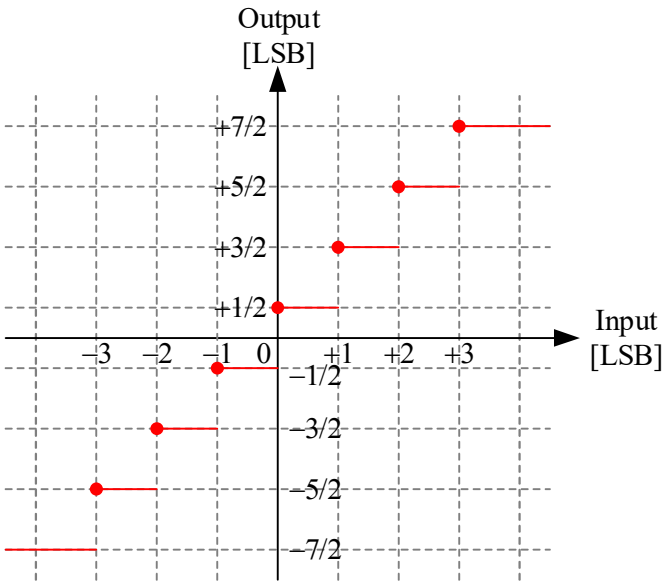

Figure 1. Input-output relation of ALMA 3-bit digitizers

Input signals are quantized by eight values (-7/2, -5/2, -3/2, -1/2, +1/2, +3/2, +5/2, +7/2) represented by (100, 101, 110, 111, 000, 001, 010, 011) in binary digits using seven threshold levels (-3, -2, -1, 0, +1, +2, +3), which are equally located. The unit is LSB (Least-Significant Bit). The eight values are transmitted to the ACA Correlator in Gray code, where they are (000, 001, 011, 010, 110, 111, 101, 100). Then, the ACA Correlator converts them into eight fixed-point values represented in 4-bit Two's complement by expanding 1-bit, which are

(1001, 1011, 1101, 1111, 0001, 0011, 0101, 0111).

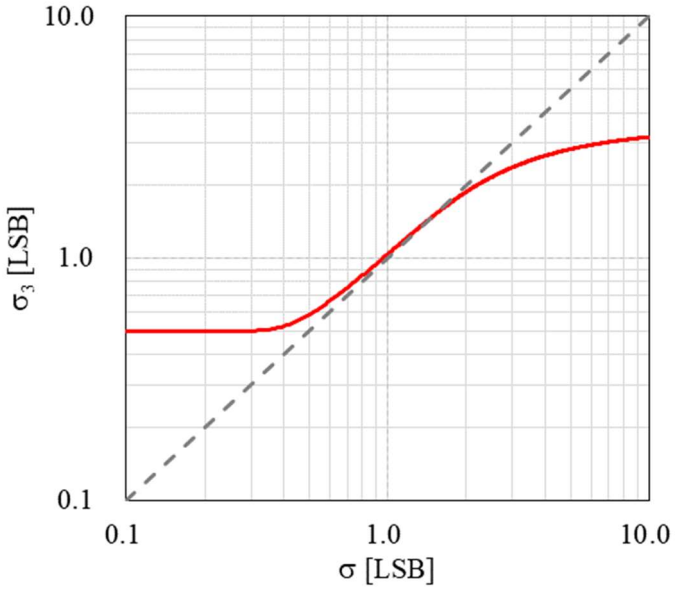

Figure 2. Nonlinear relation between input and output signal levels in the 3-bit quantization

A red-solid line shows 3-bit quantization nonlinear relation between input and output signals, whose levels are σ and σ_3 in standard deviation, respectively. The red line is calculated from the 3-bit quantization shown in Figure 1 and input signal of Gaussian noise with standard deviation of σ. A gray-dashed line indicates the linear relation between input and output signals. The red line shows the nonlinear relation, especially at higher or lower input levels. This can be explained by saturation at the higher end and uncertainty at the lower end. At the higher end, input signals that exceed the range represented by the available bits are clipped, and the output level saturates. Conversely, if the input signals are too weak and stay in the range between two thresholds, the output level is uncertain within the range and is a constant value corresponding to the range.

2. Symbols and definitions in the auto-correlation and cross-correlation corrections

Symbols and definitions are listed in Table 1. Non-quantized and 3-bit quantized time-series data correspond to inputs and outputs of 3-bit quantization, respectively, and each symbol with a suffix "3" denotes processing results of 3-bit quantized time-series data. Then, auto/cross-power spectra of time-series data with and without 3-bit quantization, $X(f)$ and $Y(f)$, are represented by Fourier transform of correlation lag of the same time-series data with and without 3-bit quantization, $l_3(\tau)$ and $l(\tau)$, respectively.

Table 1. Symbols and definitions in the two corrections

n	:	Number of samples
i, j	:	Suffixes to represent Antenna-i and Antenna-j
$l_3(\tau)$	:	Correlation lag of 3-bit quantized time-series data
	:	$l_3(\tau) = \sum_t x_{3i}(t) x_{3j}(t-\tau)$
$l(\tau)$	:	Correlation lag of non-quantized time-series data
	:	$l(\tau) = \sum_t x_i(t) x_j(t-\tau)$
$\sigma_{3(i,j)}$	:	Standard deviation of 3-bit quantized time-series data
	:	$\sigma_{3(i,j)} = \sqrt{\frac{1}{n-1}\sum_t^n x_{3(i,j)}^2(t)}$
$\sigma_{i,j}$	:	Standard deviation of non-quantized time-series data
	:	$\sigma_{i,j} = \sqrt{\frac{1}{n-1}\sum_t^n x_{i,j}^2(t)}$
$\rho_3(\tau)$	:	Correlation coefficient of 3-bit quantized time-series data
	:	$\rho_3(\tau) = \frac{\sum_t x_{3i}(t) x_{3j}(t-\tau)}{\sqrt{\frac{1}{n-1}\sum_t^n x_{3i}^2(t)}\sqrt{\frac{1}{n-1}\sum_t^n x_{3j}^2(t)}} = \frac{l_3(\tau)}{\sigma_{3i}\sigma_{3j}}$ (1)
$\rho(\tau)$	:	Correlation coefficient of non-quantized time-series data
	:	$\rho(\tau) = \frac{\sum_t x_i(t) x_j(t-\tau)}{\sqrt{\frac{1}{n-1}\sum_t^n x_i^2(t)}\sqrt{\frac{1}{n-1}\sum_t^n x_j^2(t)}} = \frac{l(\tau)}{\sigma_i\sigma_j}$ (2)
$\mathcal{F}$	:	Fourier transform
$X(f)$	:	Power spectra of 3-bit quantized time-series data $(= \mathcal{F}[l_3(\tau)])$
$Y(f)$	:	Power spectra of non-quantized time-series data $(= \mathcal{F}[l(\tau)])$

In addition, the following two functions, $Q_{3\sigma}^{-}$ and $Q_{3\rho}^{+}$, are introduced. $Q_{3\sigma}^{-}$ shows a ratio between input and output signal voltage levels (σ and σ_3) of the 3-bit quantization at an output signal voltage level (σ_3), and they (σ and σ_3) follow the relation shown in Figure 2. $Q_{3\rho}^{+}$ shows a ratio between input and output correlation coefficients (ρ and ρ_3) of the 3-bit quantization at input signal voltage levels (σ_i and σ_j). The relation between the input and output correlation

coefficients are plotted in Figure 3.

Table 1. continued

$Q_{3\sigma}^{-}[\sigma_3] \stackrel{\text{def}}{=} \frac{\sigma}{\sigma_3}$	(3)
$Q_{3\rho}^{+}[\sigma_i, \sigma_j, \rho(\tau)] \stackrel{\text{def}}{=} \frac{\rho_3(\tau)}{\rho(\tau)}$	(4)

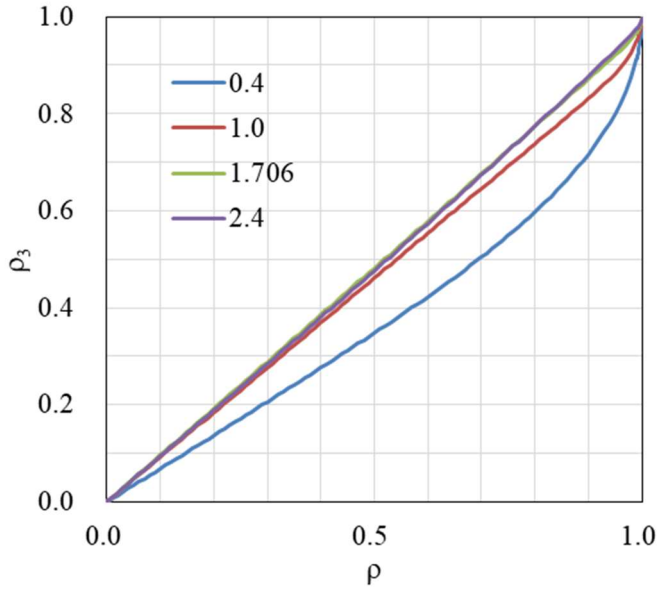

Figure 3. Nonlinear relation between input and output correlation coefficients in the 3-bit quantization

Lines show nonlinear relations between input (ρ) and output (ρ_3) correlation coefficients in the 3-bit quantization. Blue, red, green, and violet lines correspond to signal levels $\sigma(=\sigma_i=\sigma_j)$ of 0.4, 1.0, 1.706, and 2.4 input to the 3-bit quantization, respectively.

3. Auto-correlation correction for auto-power spectra in the spectral domain

In this section, we derive the relation between auto-power spectra of time-series data with and without the 3-bit quantization based on conventional quantization correction in the lag domain. In the case of auto-power spectra, since antenna-*i* and antenna-*j* are identical, the symbols in Table 1 can be represented as listed in Table 2.

Table 2. Symbols in the auto-correlation correction

$i = j$
Hence,

$$\sigma_{3i} = \sigma_{3j} \stackrel{\text{def}}{\equiv} \sigma_3$$

$$\sigma_i = \sigma_j \stackrel{\text{def}}{\equiv} \sigma$$

$$l_3(0) = \sum_t x_{3i}(t)x_{3j}(t) = \sum_t x_3^2(t) = \sigma_3^2 \tag{5}$$

$$l(0) = \sum_t x_i(t)x_j(t) = \sum_t x^2(t) = \sigma^2 \tag{6}$$

$$\frac{l(0)}{l_3(0)} = \frac{\sigma^2}{\sigma_3^2} = \{Q_{3\sigma}^-[\sigma_3]\}^2 \quad (\because (3), (5), \text{and } (6)) \tag{7}$$

$$Q_{3\rho}^+[\sigma_i, \sigma_j, \rho(\tau)] = Q_{3\rho}^+[\sigma, \rho(\tau)] = \frac{\rho_3(\tau)}{\rho(\tau)} = \frac{l_3(\tau)}{\sigma_3^2} \cdot \frac{\sigma^2}{l(\tau)} \quad (\because (1) \text{ and } (2))$$

$$= \frac{l_3(\tau)}{l_3(0)} \cdot \frac{l(0)}{l(\tau)} \quad (\because (5) \text{ and } (6)) \tag{8}$$

Auto-power spectra of non-quantized time-series data, $Y(f)$, are represented by Fourier transform of correlation lag of the same data, $l(\tau)$. Then, we try to replace $l(\tau)$ with $l_3(\tau)$ using the symbols and relations listed in Table 2 and the assumption of low correlation coefficients.

$$Y(f) = \mathcal{F}[l(\tau)]$$

$$= \sum_{\tau=0}^{N-1} l(\tau) e^{-i\frac{2\pi f\tau}{N}}$$

$$= l(0)\left\{1 + \sum_{\tau=1}^{N-1} \frac{l(\tau)}{l(0)} e^{-i\frac{2\pi f\tau}{N}}\right\}$$

$$= l(0)\left\{1 + \sum_{\tau=1}^{N-1} \frac{1}{Q_{3\rho}^+[\sigma, \rho(\tau)]} \cdot \frac{l_3(\tau)}{l_3(0)} e^{-i\frac{2\pi f\tau}{N}}\right\} \quad (\because (8))$$

$$\approx \{Q_{3\sigma}^-[\sigma_3]\}^2 l_3(0)\left\{1 + \sum_{\tau=1}^{N-1} \frac{1}{Q_{3\rho}^+[\sigma, 0]} \cdot \frac{l_3(\tau)}{l_3(0)} e^{-i\frac{2\pi f\tau}{N}}\right\} \quad (\because (7))$$

$$\left(\begin{array}{c} \because Q_{3\rho}^+[\sigma, \rho(\tau)] \approx Q_{3\rho}^+[\sigma, 0] \text{ assumming } \rho(\tau) \ll 1 \text{ at } \tau \geq 1 \\ \text{Note } \rho(\tau) = 1 \text{ at } \tau = 0 \\ \text{See also Appendix A} \end{array}\right)$$

$$= \{Q_{3\sigma}^-[\sigma_3]\}^2 \left\{\left(1 - \frac{1}{Q_{3\rho}^+[\sigma, 0]}\right) l_3(0) + \frac{1}{Q_{3\rho}^+[\sigma, 0]} \sum_{\tau=0}^{N-1} l_3(\tau) e^{-i\frac{2\pi f\tau}{N}}\right\}$$

$$= \frac{\{Q_{3\sigma}^{-}[\sigma_3]\}^2}{Q_{3\rho}^{+}[\sigma,0]}\{(Q_{3\rho}^{+}[\sigma,0]-1)\sigma_3^2 + \mathcal{F}[l_3(\tau)]\}$$

$$= \frac{\{Q_{3\sigma}^{-}[\sigma_3]\}^2}{Q_{3\rho}^{+}[\sigma,0]}\{(Q_{3\rho}^{+}[\sigma,0]-1)\sigma_3^2 + X(f)\} \quad (9)$$

$$(\text{where } \sigma = Q_{3\sigma}^{-}[\sigma_3]\cdot\sigma_3)$$

Eq. (9) indicates that the relation between input and output spectra, $X(f)$ and $Y(f)$, is a linear function whose inclination and Y-intercept are $\frac{\{Q_{3\sigma}^{-}[\sigma_3]\}^2}{Q_{3\rho}^{+}[\sigma,0]}$ and $\frac{\{Q_{3\sigma}^{-}[\sigma_3]\}^2}{Q_{3\rho}^{+}[\sigma,0]}(Q_{3\rho}^{+}[\sigma,0]-1)\sigma_3^2$, respectively. They also indicate that the function depends on total-power input to the 3-bit quantization.

4. Cross-correlation correction for cross-power spectra in the spectral domain

In this section, we derive the relation between cross-power spectra of time-series data with and without the 3-bit quantization as well as Section 3. In the case of cross-power spectra, since antenna-*i* and antenna-*j* are different, the symbols in Table 1 can be represented as listed in Table 3. Different from auto-power spectra, $l(0)$ and $l_3(0)$ don't correspond to total power of input and output signals in the 3-bit quantization, respectively. Neither $\rho(0)$ nor $\rho_3(0)$ are equal to 1.

Table 3. Symbols in the cross-correlation correction

$i \neq j$

$$l_3(0) = \frac{\sum_t x_{3i}(t)x_{3j}(t)}{\sqrt{\frac{\sum_t^n x_{3i}^2(t)}{n-1}}\sqrt{\frac{\sum_t^n x_{3j}^2(t)}{n-1}}}\sqrt{\frac{\sum_t^n x_{3i}^2(t)}{n-1}}\sqrt{\frac{\sum_t^n x_{3j}^2(t)}{n-1}} = \rho_3(0)\sigma_{3i}\sigma_{3j} \quad (10)$$

$$l(0) = \frac{\sum_t x_i(t)x_j(t)}{\sqrt{\frac{\sum_t^n x_i^2(t)}{n-1}}\sqrt{\frac{\sum_t^n x_j^2(t)}{n-1}}}\sqrt{\frac{\sum_t^n x_i^2(t)}{n-1}}\sqrt{\frac{\sum_t^n x_j^2(t)}{n-1}} = \rho(0)\sigma_i\sigma_j \quad (11)$$

$$\frac{l(0)}{l_3(0)} = \frac{\rho(0)\sigma_i\sigma_j}{\rho_3(0)\sigma_{3i}\sigma_{3j}} = \frac{Q_{3\sigma}^{-}[\sigma_{3i}]\cdot Q_{3\sigma}^{-}[\sigma_{3j}]}{Q_{3\rho}^{+}[\sigma_i,\sigma_j,\rho(0)]} \quad (\because (3), (4), (10), \text{and } (11)) \quad (12)$$

$$Q_{3\rho}^{+}[\sigma_i,\sigma_j,\rho(\tau)] = \frac{\rho_3(\tau)}{\rho(\tau)} = \frac{l_3(\tau)}{\sigma_{3i}\sigma_{3j}}\cdot\frac{\sigma_i\sigma_j}{l(\tau)} \quad (\because (1) \text{ and } (2))$$

$$= Q_{3\rho}^{+}\left[\sigma_i, \sigma_j, \rho(0)\right] \cdot \frac{l_3(\tau)}{l_3(0)} \cdot \frac{l(0)}{l(\tau)} \quad (\because (4)) \tag{13}$$

Cross-power spectra of non-quantized time-series data, $Y(f)$, are also represented by Fourier transform of correlation lag of the same data, $l(\tau)$. Then, we try to replace $l(\tau)$ with $l_3(\tau)$ using the symbols and relations listed in Table 3 and the assumption of low correlation coefficients as well as auto-power spectra. In the case of cross-power spectra, it is unnecessary to separate $\tau = 0$ from $\tau \geq 1$ because of $\rho(\tau = 0) \ll 1$. They, however, are presented separately in the following equations for comparison with auto-power spectra.

$$Y(f) = \mathcal{F}[l(\tau)]$$

$$= \sum_{\tau=0}^{N-1} l(\tau) e^{-i\frac{2\pi f \tau}{N}}$$

$$= l(0)\left\{1 + \sum_{\tau=1}^{N-1} \frac{l(\tau)}{l(0)} e^{-i\frac{2\pi f \tau}{N}}\right\}$$

$$= l(0)\left\{1 + \sum_{\tau=1}^{N-1} \frac{Q_{3\rho}^{+}\left[\sigma_i, \sigma_j, \rho(0)\right]}{Q_{3\rho}^{+}\left[\sigma_i, \sigma_j, \rho(\tau)\right]} \cdot \frac{l_3(\tau)}{l_3(0)} e^{-i\frac{2\pi f \tau}{N}}\right\} \quad (\because (13))$$

$$\approx \frac{Q_{3\sigma}^{-}[\sigma_{3i}] \cdot Q_{3\sigma}^{-}[\sigma_{3j}]}{Q_{3\rho}^{+}\left[\sigma_i, \sigma_j, 0\right]} l_3(0)\left\{1 + \sum_{\tau=1}^{N-1} \frac{l_3(\tau)}{l_3(0)} e^{-i\frac{2\pi f \tau}{N}}\right\} \quad (\because (12))$$

$$\left(\because Q_{3\rho}^{+}\left[\sigma_i, \sigma_j, \rho(\tau)\right] \approx Q_{3\rho}^{+}\left[\sigma_i, \sigma_j, 0\right] \text{ assumming } \rho(\tau) \ll 1 \text{ at } \tau \geq 0 \right.$$
$$\left. \text{See also Appendix A} \right)$$

$$= \frac{Q_{3\sigma}^{-}[\sigma_{3i}] \cdot Q_{3\sigma}^{-}[\sigma_{3j}]}{Q_{3\rho}^{+}\left[\sigma_i, \sigma_j, 0\right]}\left\{(1-1) l_3(0) + \sum_{\tau=0}^{N-1} l_3(\tau) e^{-i\frac{2\pi f \tau}{N}}\right\} \quad (\because (12))$$

$$= \frac{Q_{3\sigma}^{-}[\sigma_{3i}] \cdot Q_{3\sigma}^{-}[\sigma_{3j}]}{Q_{3\rho}^{+}\left[\sigma_i, \sigma_j, 0\right]} \mathcal{F}[l_3(\tau)]$$

$$= \frac{Q_{3\sigma}^{-}[\sigma_{3i}] \cdot Q_{3\sigma}^{-}[\sigma_{3j}]}{Q_{3\rho}^{+}\left[\sigma_i, \sigma_j, 0\right]} X(f) \tag{14}$$

$$\left(\text{where } \sigma_{i,j} = Q_{3\sigma}^{-}\left[\sigma_{3(i,j)}\right] \cdot \sigma_{3(i,j)}\right)$$

Similar to Eq. (9), Eq. (14) indicates that the relation between input and output spectra, $X(f)$

and $Y(f)$, is a simple linear function of $Y(f) = \alpha X(f)$, where α is $\frac{Q_{3\sigma}^{-}[\sigma_{3i}] \cdot Q_{3\sigma}^{-}[\sigma_{3j}]}{Q_{3\rho}^{+}[\sigma_i, \sigma_j, 0]}$. It is noted that $X(f)$ and $Y(f)$ are not normalized by relevant auto-correlation spectra and that their phases remain the same.

5. Computational simulation of the auto-correlation and cross-correlation corrections

In the previous sections, we have derived the linear relations between input and output spectra of the 3-bit quantization as shown in Eq. (9) and Eq. (14) assuming low correlation coefficients of $\rho \ll 1$. Next, we verify the linear relations represented by Eq. (9) and Eq. (14) using computationally generated spectra and confirm that input spectra can be recovered from output spectra distorted by the 3-bit quantization with the relations. In the verification, the two functions, $Q_{3\sigma}^{-}[\sigma_3]$ and $Q_{3\rho}^{+}[\sigma_i, \sigma_j, 0]$, are computationally calculated using Mathematica, and their interpolated functions by cubic spline functions are used (see Appendix B for $Q_{3\sigma}^{-}[\sigma_3]$ and Appendix C for $Q_{3\rho}^{+}[\sigma_i, \sigma_j, 0]$).

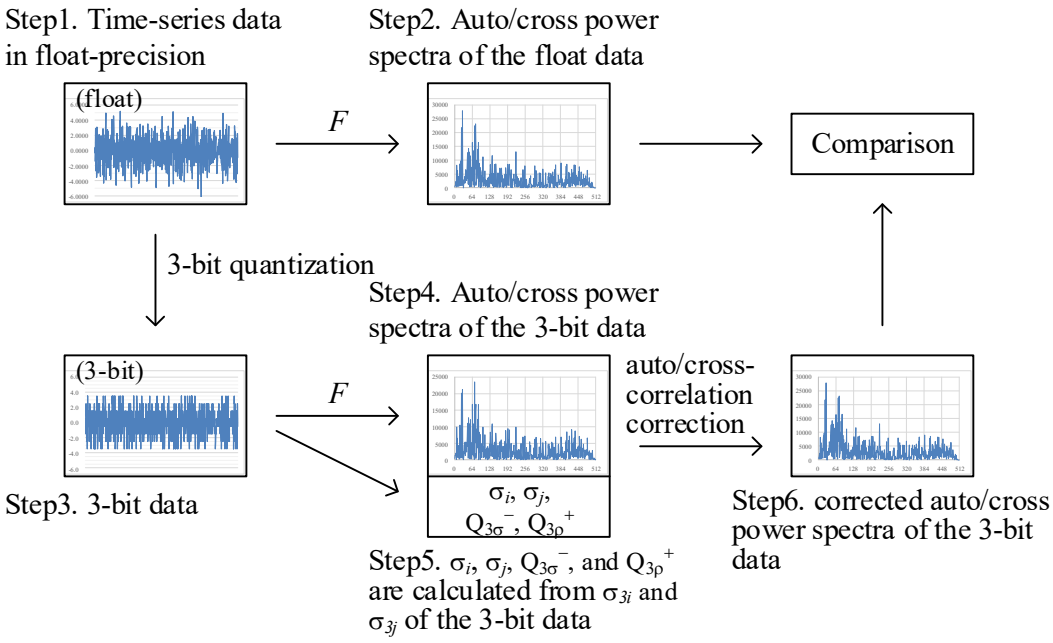

Figure 4. Verification procedures of the auto/cross-correlation correction

Time-series data are computationally generated in float-precision and quantized by 3-bit. The auto/cross-power spectra of the float and 3-bit data are calculated using FFT, and then, the auto/cross-correlation correction is applied to the spectra of the 3-bit data. Finally, the float and corrected 3-bit spectra are compared with each other.

The verification is done in the following steps, which are shown in Figure 4.

Step 1. Time-series data are computationally generated in float-precision.

Step 2. Auto/cross power spectra, corresponding to $Y(f)$ in Eq. (9)/ Eq. (14), are calculated from the time-series data using 1024-point Fast Fourier Transform (FFT).

Step 3. The time-series data are computationally quantized by 3-bit.

Step 4. Auto/cross-power spectra, corresponding to $X(f)$ in Eq. (9)/ Eq. (14), are calculated from the 3-bit time-series data.

Step 5. Standard deviation σ_i and σ_j of the float time-series data are estimated from standard deviation σ_{3i} and σ_{3j} of the 3-bit time-series data using the $Q_{3\sigma}^{-}[\sigma_3]$ function, and then, correction parameters are derived from σ_i, σ_j, and the $Q_{3\rho}^{+}[\sigma_i, \sigma_j, 0]$ function.

Step 6. The auto/cross-correlation correction is applied to $X(f)$, and corrected $X(f)$ is compared with $Y(f)$.

Hereafter, we present four cases of auto and cross power spectra with various total-power levels input to the 3-bit quantization.

Case 1. Auto power spectra with optimal total-power level input to the 3-bit quantization

This is a case of auto-power spectra whose total-power levels input to the 3-bit quantization are optimal for the quantization like target observations with ALMA on the sky including science targets and calibrators. Table 4 lists statistics and level histogram of generated float and 3-bit time-series data. Figure 5 shows auto-power spectra of the two data, amplitude comparison between the two spectra, a corrected 3-bit spectrum using the auto-correlation correction, and differences between the corrected 3-bit and original float spectra. These plots confirm that there is the linear relation represented by Eq. (9) between input and output auto-power spectra in the 3-bit quantization. They also confirm that the relation can recover original auto-power spectra from distorted auto-power spectra due to the 3-bit quantization.

Table 4. Statistics and level histogram of generated float and 3-bit data

Statistics of time-series data							
	Number of samples	Mean	Standard deviation	Maximum values	Minimum values		
Float data	67108864	+0.014	1.712	+10.150	-9.616		
3-bit data		+0.014	1.678	+3.5	-3.5		
Level histogram of 3-bit data [%]							
x<−3	−3≤x<−2	−2≤x<−1	−1≤x<0	0≤x<+1	+1≤x<+2	+2≤x<+3	+3≤ x

3.9	8.1	15.7	22.0	22.1	15.9	8.2	4.1

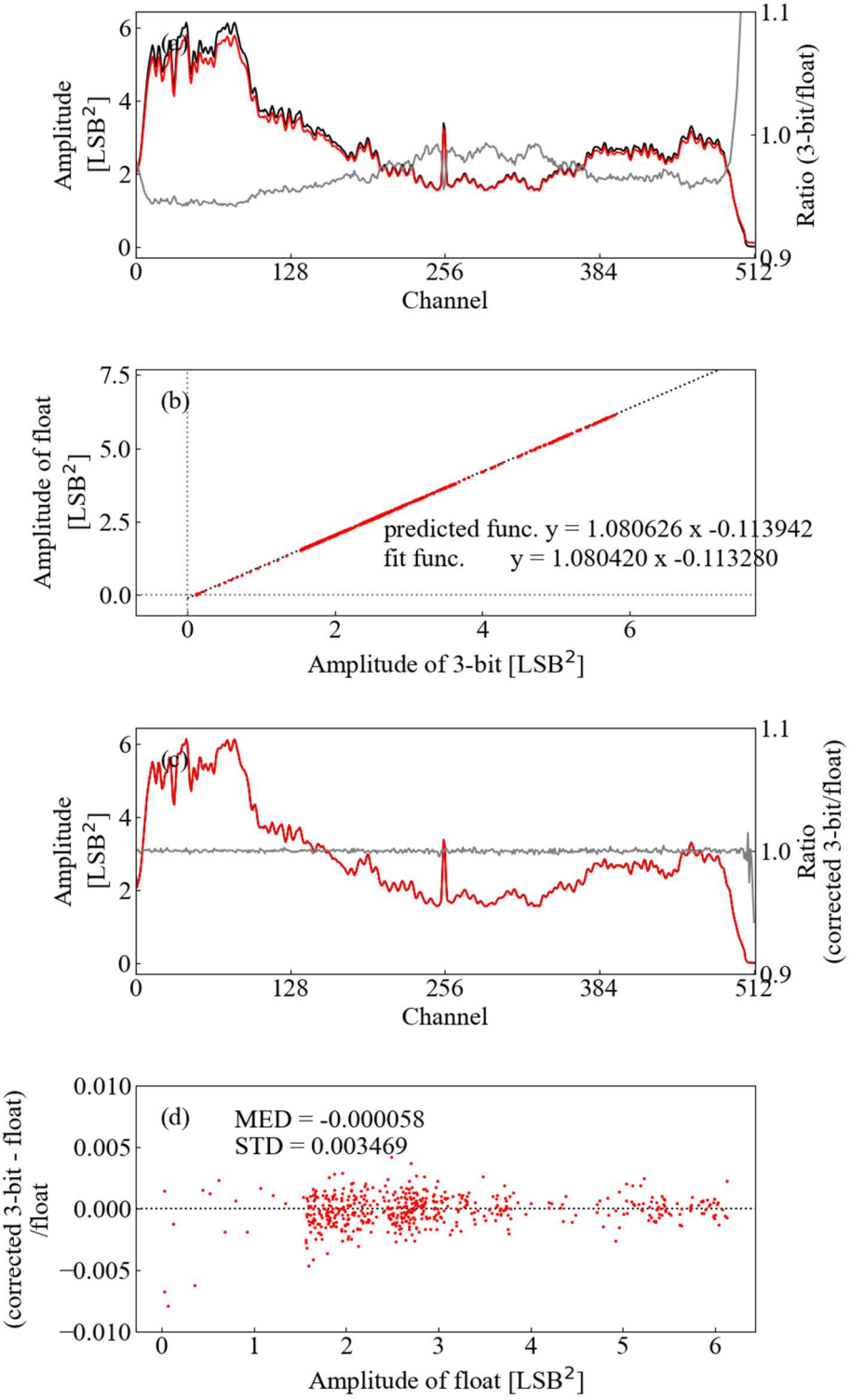

Figure 5. Comparison between the corrected 3-bit and float spectra

(a) Auto-power spectra of time-series data in 3-bit (red line) and float (black line) precisions.

The righthand y-axis corresponds to the gray line, which shows ratios between the two spectra. (b) Amplitudes of the two spectra are plotted by red dots to confirm the linear relation (black dot line) predicted from Eq. (9). The two equations in the plot show function parameters predicted from Eq. (9) and derived from a linear fit to the red dots. (c) The corrected auto-power spectrum (red line) of the 3-bit data using Eq. (9). The spectrum is compared with the auto-power spectrum of the float data (black line). As shown in a gray line of their ratios, the two spectra agree with each other, and the black line is coincident with the red line. (d) Differences between the corrected 3-bit and float spectra are normalized by the float spectrum and plotted as red dots at each amplitude of the float spectrum. Their median and standard deviation are also shown in the plot.

Case 2. Auto power spectra with high total-power level input to the 3-bit quantization

This is a case of auto-power spectra whose total-power levels input to the 3-bit quantization are not optimal like hot-load measurements at atmospheric calibration in ALMA. Table 5 lists statistics and level histogram of generated float and 3-bit time-series data. Figure 6 also confirms the linear relation of Eq. (9) and successful auto-correlation correction in auto-power spectra as well as Case 1.

Table 5. Statistics and level histogram of generated float and 3-bit data

Statistics of time-series data							
	Number of samples	Mean	Standard deviation	Maximum values	Minimum values		
Float data	67108864	-0.005	2.424	+14.400	-13.877		
3-bit data		-0.004	2.131	+3.5	-3.5		
Level histogram of 3-bit data [%]							
x<−3	−3≤x<−2	−2≤x<−1	−1≤x<0	0≤x<+1	+1≤x<+2	+2≤x<+3	+3≤ x
10.8	9.7	13.5	16.0	16.0	13.5	9.7	10.8

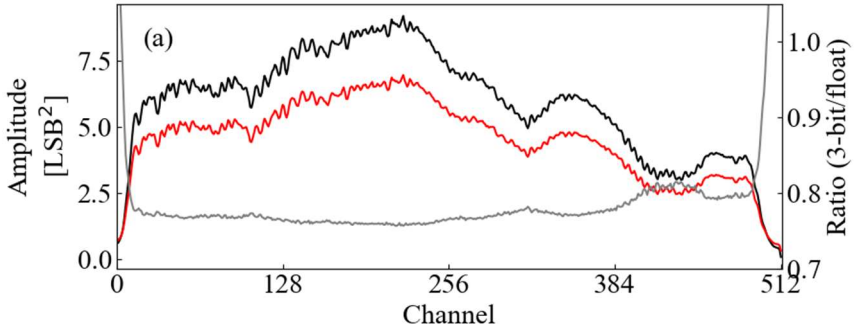

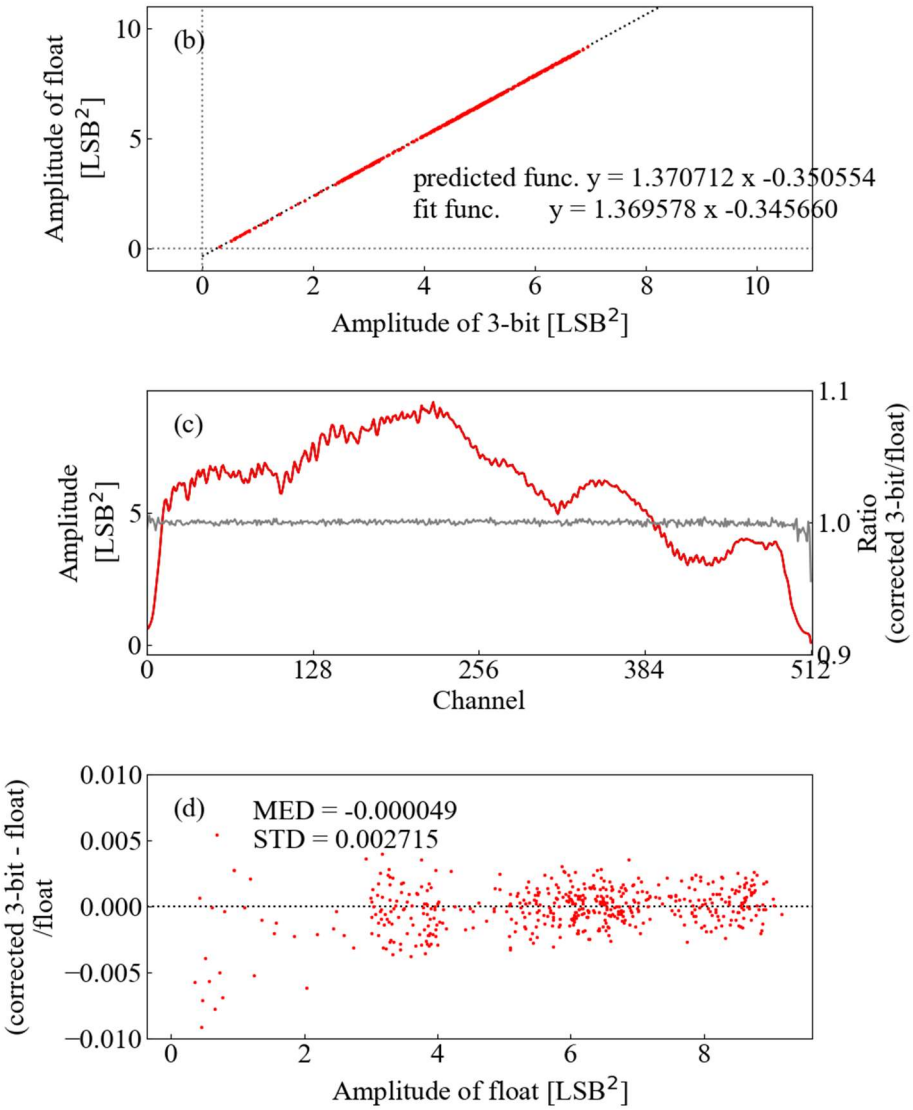

Figure 6. Comparison between the corrected 3-bit and float spectra

Same as Figure 5, but a different signal level input to the 3-bit quantization. The 2nd plot shows that amplitudes of the two spectra can be represented by the linear relation predicted from Eq. (9) as well as Figure 5b.

<u>Case 3. Cross power spectra with optimal total-power levels input to the 3-bit quantization</u>

This is a case of cross-power spectra like target observations with ALMA which contain a celestial point-source at the phase center with a thermally-excited spectral line of FWHM ~60 channels, where total-power levels input to 3-bit quantization are optimal for the quantization. Table 6 lists statistics and level histograms of generated float and 3-bit time-series data. Figure 7 shows cross-power spectra of the two data, amplitude comparison between the two spectra, a corrected 3-bit spectrum using the cross-correlation correction, and differences between the corrected 3-bit and

original float spectra. These plots confirm the linear relation of Eq. (14) between input and output cross-power spectra in the 3-bit quantization and the recovery of original cross-power spectra from distorted cross-power spectra due to the 3-bit quantization using the relation.

Table 6. Statistics and level histograms of generated float and 3-bit data

Statistics of time-series data								
Data	Number of samples			Mean	Standard deviation	Maximum values	Minimum values	
Float_i	163840000			0.000	1.691	+9.422	-9.944	
Float_j				0.000	1.735	+9.701	-9.790	
3-bit_i				0.000	1.662	+3.5	-3.5	
3-bit_j				0.000	1.696	+3.5	-3.5	
Level histogram of time-series 3-bit data [%]								
	x<−3	−3≤x<−2	−2≤x<−1	−1≤x<0	0≤x<+1	+1≤x<+2	+2≤x<+3	+3≤ x
3-bit_i	3.8	8.0	15.9	22.3	22.3	15.9	8.0	3.8
3-bit_j	4.2	8.3	15.8	21.8	21.8	15.8	8.3	4.2

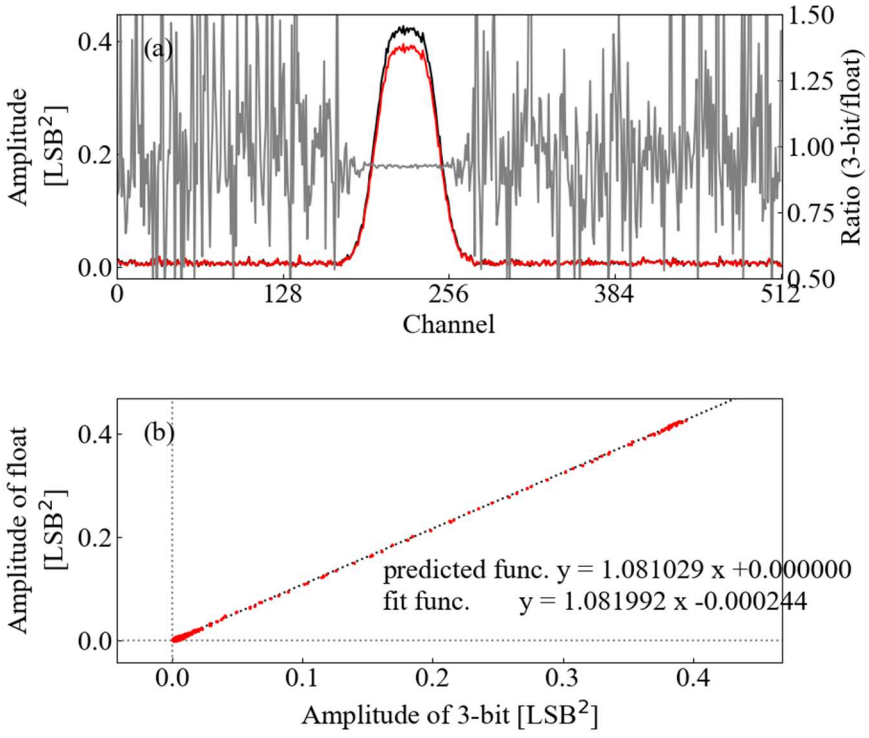

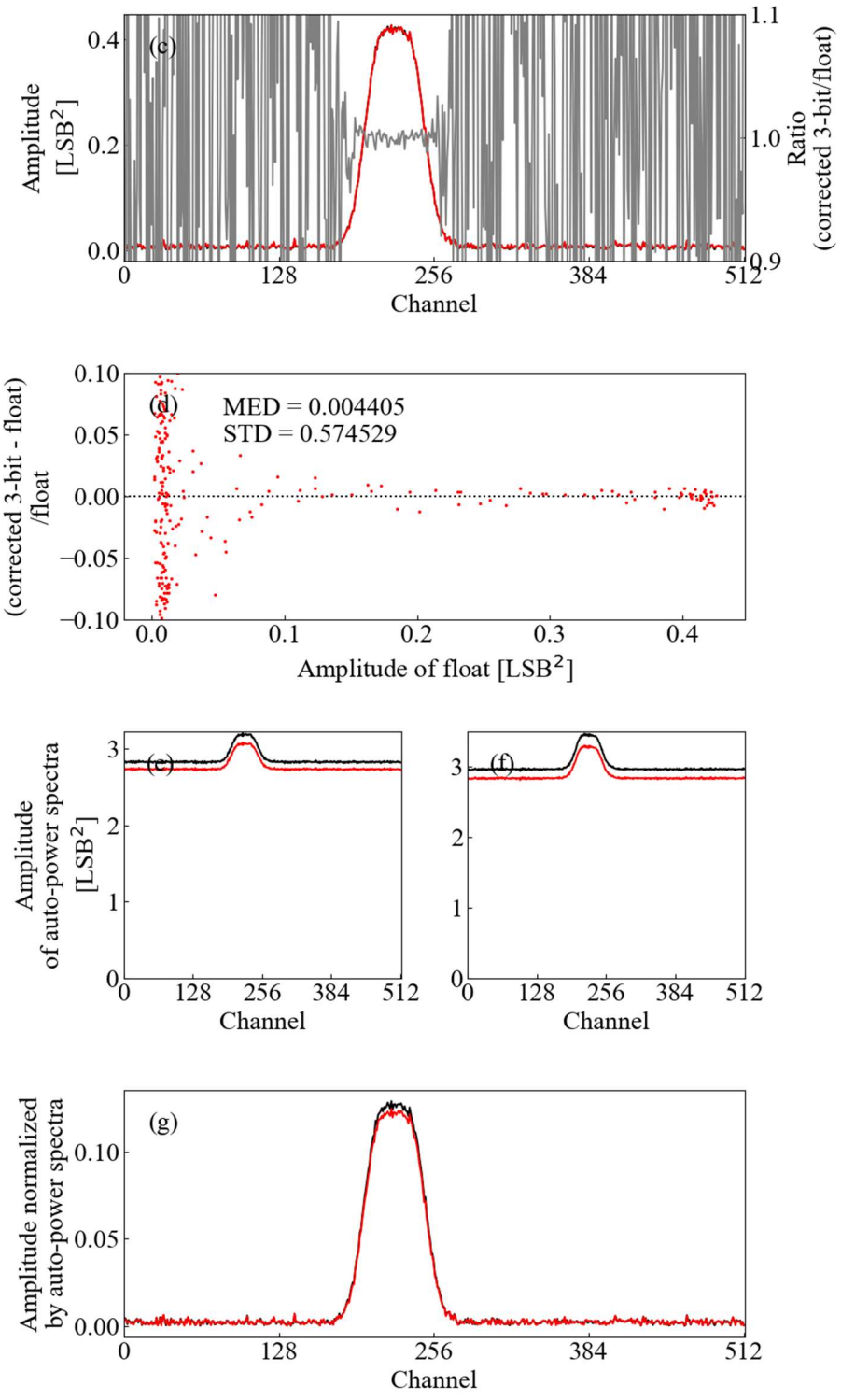
(c)
Amplitude [LSB^2]
Ratio (corrected 3-bit/float)
Channel
(d)
MED = 0.004405
STD = 0.574529
(corrected 3-bit - float) /float
Amplitude of float [LSB^2]
(e)
(f)
Amplitude of auto-power spectra [LSB^2]
Channel
(g)
Amplitude normalized by auto-power spectra
Channel

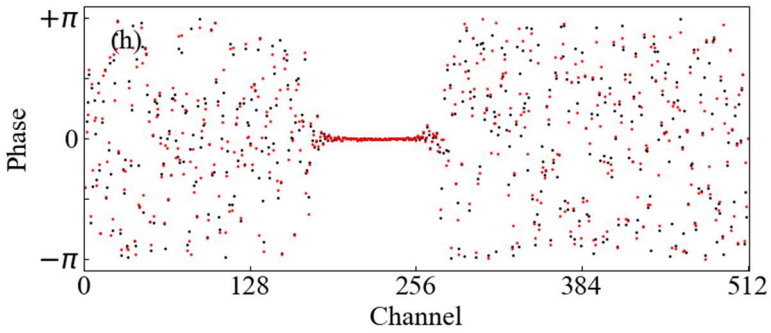

Figure 7. Comparison between the corrected 3-bit and float spectra

(a) Cross-power spectra of time-series data in 3-bit (red line) and float (black line) precisions. The righthand y-axis corresponds to the gray line, which shows ratios between the two spectra. (b) Amplitudes of the two spectra are plotted by red dots to confirm the linear relation (black dot line) predicted from Eq. (14). The two equations in the plot show function parameters that are predicted from Eq. (14) and derived from a linear fit to the red dots. (c) The corrected cross-power spectrum (red line) of the 3-bit data using Eq. (14). The spectrum is compared with the cross-power spectrum of the float data (black line). As shown in a gray line of their ratios, the two spectra agree with each other, and the black line is coincident with the red line. (d) Differences between the corrected 3-bit and float spectra are normalized by the float spectrum and plotted as red dots at each amplitude of the float spectrum. Their median and standard deviation are also shown in the plot. (e) and (f) Two auto-power spectra of the 3-bit (red line) and float (black line) data. (g) and (h) Amplitudes and phases of the cross-power spectra (a) normalized by two auto-power spectra (e) and (f). Red and black lines correspond to the 3-bit and float data, respectively.

Case 4. Cross power spectra with different total-power levels input to the 3-bit quantization

This is a case of cross-power spectra containing two different celestial spectral lines whose FWHMs are ~30 and ~90 channels, where total-power levels input to 3-bit quantization are not optimal for the quantization. Table 7 lists statistics and level histograms of generated float and 3-bit time-series data. Figure 8 also confirms the linear relation of Eq. (14) and successful cross-correlation correction in cross-power spectra as well as Case 3.

Table 7. Statistics and level histograms of generated float and 3-bit data

Statistics of time-series data					
Data	Number of samples	Mean	Standard deviation	Maximum values	Minimum values
Float [i]	163840000	0.000	1.458	+9.454	-9.941

Float [j]				0.000	1.965	+12.498	-13.845	
3-bit [i]				0.000	1.467	+3.5	-3.5	
3-bit [j]				0.000	1.861	+3.5	-3.5	
Level histogram of time-series 3-bit data [%]								
	x<−3	−3≤x<−2	−2≤x<−1	−1≤x<0	0≤x<+1	+1≤x<+2	+2≤x<+3	+3≤ x
3-bit [i]	2.0	6.5	16.1	25.4	25.4	16.1	6.5	2.0
3-bit [j]	6.3	9.1	15.1	19.5	19.5	15.1	9.1	6.3

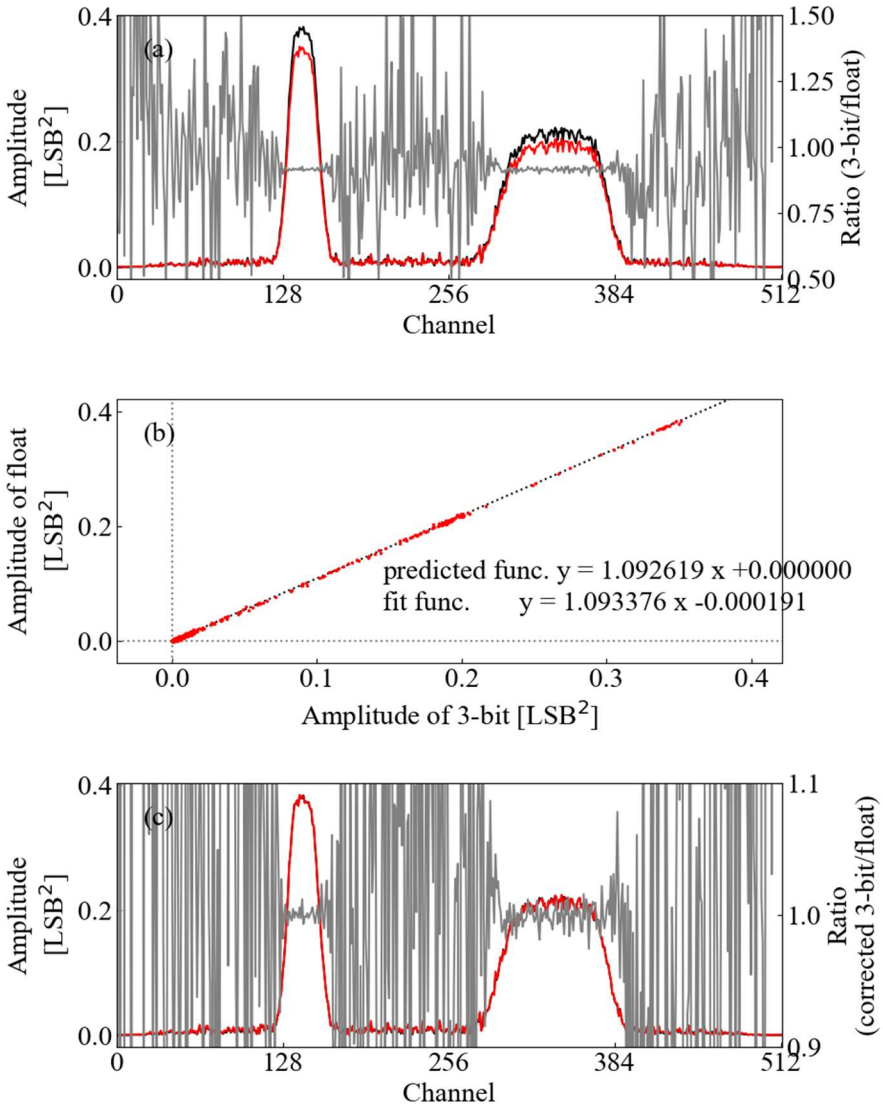

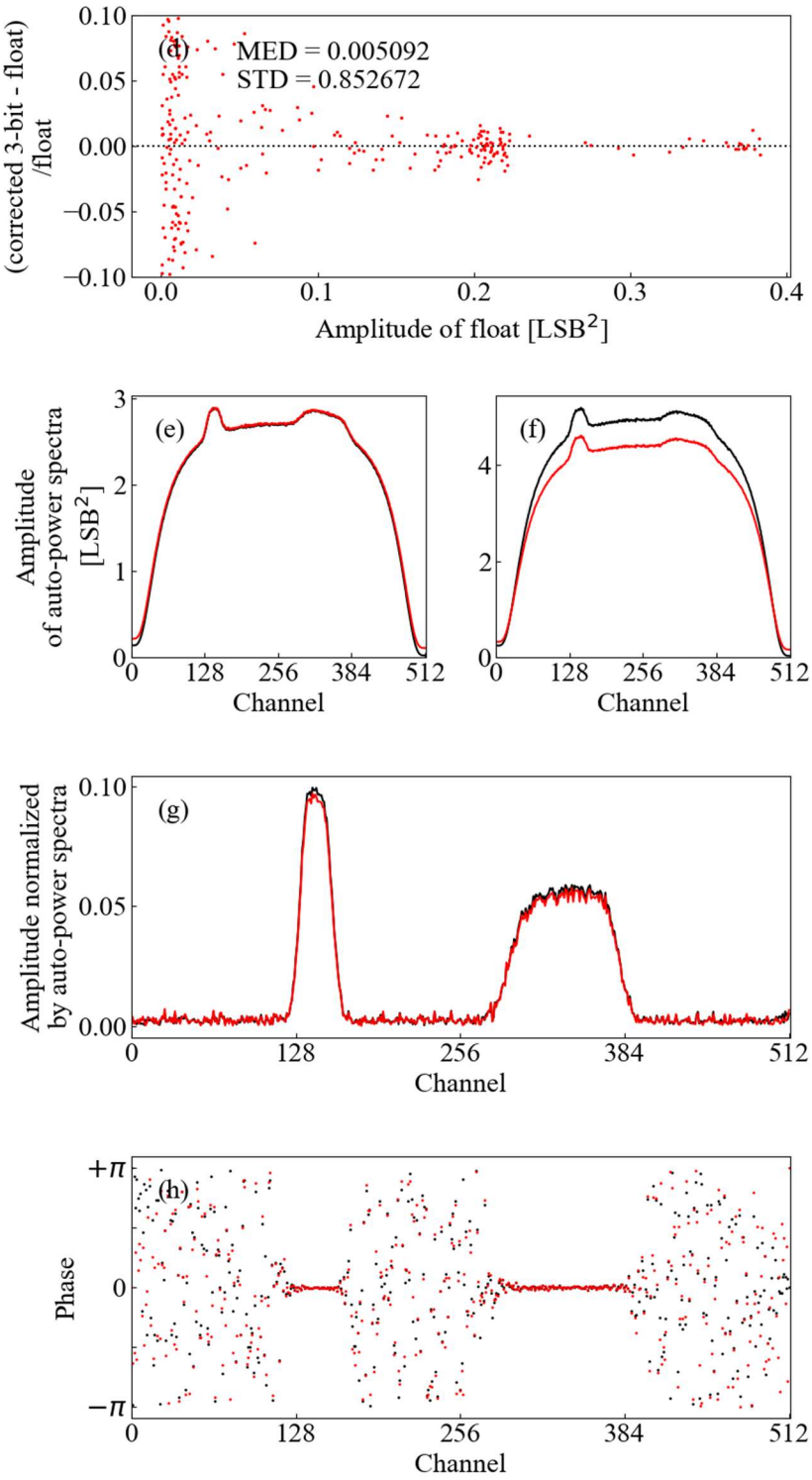

Figure 8. Comparison between the corrected 3-bit and float spectra

Same as Figure 7, but different signals input to the 3-bit quantization. The 2nd plot shows the linear relation of Eq. (14) between input and output spectra in the 3-bit quantization as well as Figure 7b.

6. Summary

We have analytically derived the linear relations between input and output auto/cross-power spectra of the 3-bit quantization assuming low correlation coefficients of time-series data. Then, the auto/cross-correlation correction using the relations is applied to auto/cross-power spectra of 3-bit time-series data, which are computationally generated in float-precision and quantized by 3-bit. The corrected auto/cross-power spectra agree with those of original float time-series data, and we have confirmed the linear relations and the recovery of original spectra using the relations in both of auto and cross-power spectra.

Since the linear relations of the auto/cross-power spectra depend on signal levels input to the 3-bit digitizers, the auto/cross-correlation correction factors need to be updated at the timing of the level changes. This usually corresponds to integration duration of data dumped from a correlator or a spectrometer, because such level changes come from bright targets (e.g., cross-scan of calibrators such as planets, on-the-fly observations toward massive star forming regions) and time-variations in atmosphere and instrument conditions (e.g., system temperature measurements using the chopper-wheel method, elevation changes).

The proposed correction was originally developed for the ACA Correlator employing FX architecture to process 3-bit quantization correction. The correction is, however, not specific to the FX architecture and is applicable to other architectures such as FFX, FXF, and XF. In particular, the correction can be useful for FFX and FXF architecture correlators, because not all spectra of data input to digitizers are always output from them, and it can be difficult to apply conventional corrections in the lag domain.

In this memo, we have focused on the 3-bit quantization. The analytical study, however, does not relay on the number of quantization bits. Thus, if we prepare $Q_{n\sigma}^{-}$ and $Q_{n\rho}^{+}$ functions for n-bit quantization as well as $Q_{3\sigma}^{-}$ and $Q_{3\rho}^{+}$ for the 3-bit quantization, the auto-correlation and cross-correlation corrections are easily applicable to another n-bit quantization.

We would like to acknowledge the reviewer for constructive comments and suggestions which improve our paper. We are grateful to Todd Hunter for his constructive comments.

References

[1] Kamazaki, T., Okumura, K.S., Chikada, Y., Okuda, T., Kurono, Y., Iguchi, S., Mitsuishi, S., Murakami, Y., Nishimuta, N., Mita, H., and Sano, R., 2012, “Digital Spectro-Correlator System for the Atacama Compact Array of the Atacama Large Millimeter/Submillimeter Array”, PASJ, 64, 29

[2] Baudry, A., Deschans, D., Begueret, J., Deval, Y., Fouillat, P., Montignac, G., Gentaz, O.,

Torres, M., 2002, “Designing and Prototyping of 2-4 GHz Bandpass SiGe Digitizers and Associated Test Equipment for the ALMA Project. I”, ALMA Memo 410

[3] Recoquillon, C., Baudry, A., Begueret, J., Gauffre, S., Montignac, G., 2004, “The ALMA Digitizer (DG) Demultiplexer : Design, Performances in DG Assembly and Production Acceptance Tests”, ALMA Memo 510

[4] Escoffier, R.P., Comoretto, G., Webber, J.C., Baudry, A., Broadwell, C.M., Greenberg, J.H., Treacy, R.R., Cais, P., Quertier, B., Camino, P., Bos, A., and Gunst, A.W., 2007, “The ALMA correlator”, A&A, 462, 801

Appendix A. Ratios between input and output correlation coefficients of the 3-bit quantization

We have derived Eq. (9) and Eq. (14) assuming that ratios between input and output correlation coefficients (ρ and ρ_3) at $\rho \ll 1$ can be approximated by the ratios at $\rho = 0$ in the 3-bit quantization. For confirmation, Figure 9 shows the ratios normalized by the ratios at $\rho = 0$ depending on input correlation coefficients and input signal levels. The plot suggests that the assumption is reasonable roughly at $\rho < 0.4$, where the normalized ratios are in the range of 1.00 – 1.01, in the 3-bit quantization. In general, astronomical signals are much weaker than system noise, and the $\rho < 0.4$ condition would be available in many of radio astronomical observations. This assumption might be inappropriate when observing very narrow and extremely bright lines with low-noise systems (e.g. very bright maser sources at a centimeter wavelength).

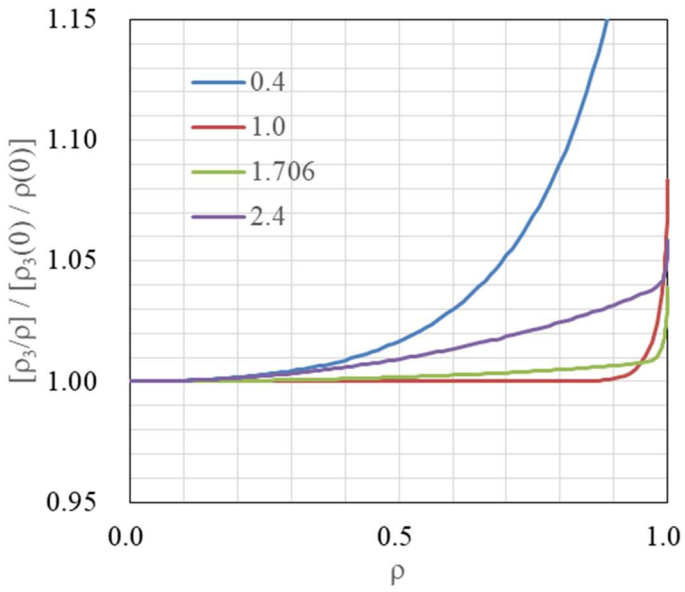

Figure 9. Ratios between input and output correlation coefficients normalized by the ratios at $\rho = 0$ in the 3-bit quantization

Ratios between input and output correlation coefficients in the 3-bit quantization are divided by the ratios at $\rho = 0$. Different colors indicate different signal levels input to the 3-bit quantization. Blue, red, green, and violet lines correspond to signal levels $\sigma\left(= \sigma_i = \sigma_j\right)$ of 0.4, 1.0, 1.706, and 2.4 input to the 3-bit quantization, respectively.

Appendix B. $Q_{3\sigma}^{-}$ function

$Q_{3\sigma}^{-}$ shows ratios between input and output signal voltage levels of the 3-bit quantization, and it is a correction function from output voltage levels to input voltage levels. The function is computationally calculated assuming input signals of Gaussian noise and the 3-bit quantization shown in Figure 1, and its values are listed in Table 8. In the computational simulation of Section 5, a cubic spline function, scipy.interpolate.CubicSpline() in Python 3, with Table 8 is used to represent the $Q_{3\sigma}^{-}$ function.

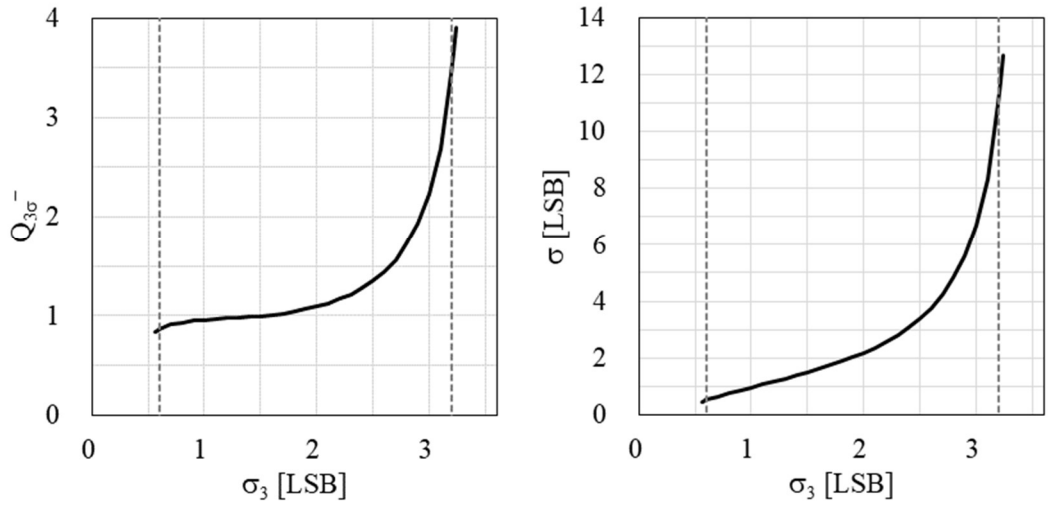

Figure 10. Computationally calculated $Q_{3\sigma}^{-}$ function

The $Q_{3\sigma}^{-}$ function (left) and σ vs. σ_3 (right) are computationally calculated and plotted by a black line. The interpolation range ($0.6 \leq \sigma_3 \leq 3.2$) of the cubic spline is shown by two vertical dashed lines.

Table 8. Computationally calculated $Q_{3\sigma}^{-}$ values

See the "ApB (Q3s-_T)" sheet in the "alma_memo629-tables.xlsx" Excel file.

Table 9. Coefficients of the cubic spline function for $Q_{3\sigma}^{-}$

See the "ApB (Q3s-_T)" sheet of the "alma_memo629-tables.xlsx" Excel file.

Table 10. Coefficients of the cubic spline function for σ vs. σ_3

See the "ApB (Q3s-_T)" sheet of the "alma_memo629-tables.xlsx" Excel file.

Appendix C. $Q_{3\rho}^{+}$ function

$Q_{3\rho}^{+}$ shows ratios between input and output correlation coefficients of the 3-bit quantization at low correlation coefficients of $\rho \ll 1$, and it is a correction function from input correlation coefficients to output correlation coefficients. The function at $\rho = 0$ is computationally calculated using Mathematica, and its values are listed in Table 11. In the computational simulation of Section 5, a linear interpolation function, scipy.interpolate.interpn() in Python3, with Table 11 is used to represent the $Q_{3\rho}^{+}$ function.

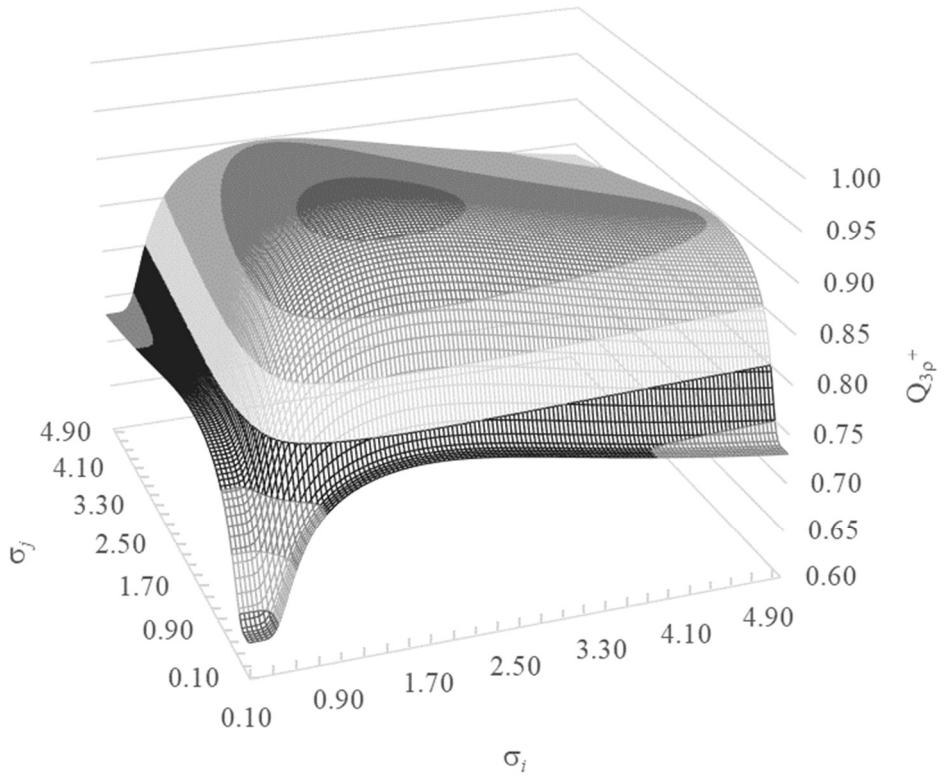

Figure 11. Computationally calculated $Q_{3\rho}^{+}$ function

The $Q_{3\rho}^{+}$ function at $\rho = 0$ is computationally calculated and shown by a surface plot. Different gray scales for the surface plot are used every 0.05 in $Q_{3\rho}^{+}$.

Table 11. Computationally calculated $Q_{3\rho}^{+}$ values

See the "ApC (Q3r+_T)" sheet in the "alma_memo629-tables.xlsx" Excel file.

Appendix D. Auto-correlation correction for the ACA Correlator

In the auto-correlation correction, also known as the linearity correction, for ACACORR, a cubic spline function (see Eq. (15) and Figure 12) is used to represent $[Q_{3\sigma}^{-}]^2$, which is a square of $Q_{3\sigma}^{-}$, and the coefficients for the cubic spline function are determined as listed in Table 13 from Table 12.

$$[Q_{3\sigma}^{-}(x)]^2 \equiv a_i(x - x_i)^3 + b_i(x - x_i)^2 + c_i(x - x_i) + d_i \quad (15)$$
$$(\text{where } x = \sigma_3^2)$$

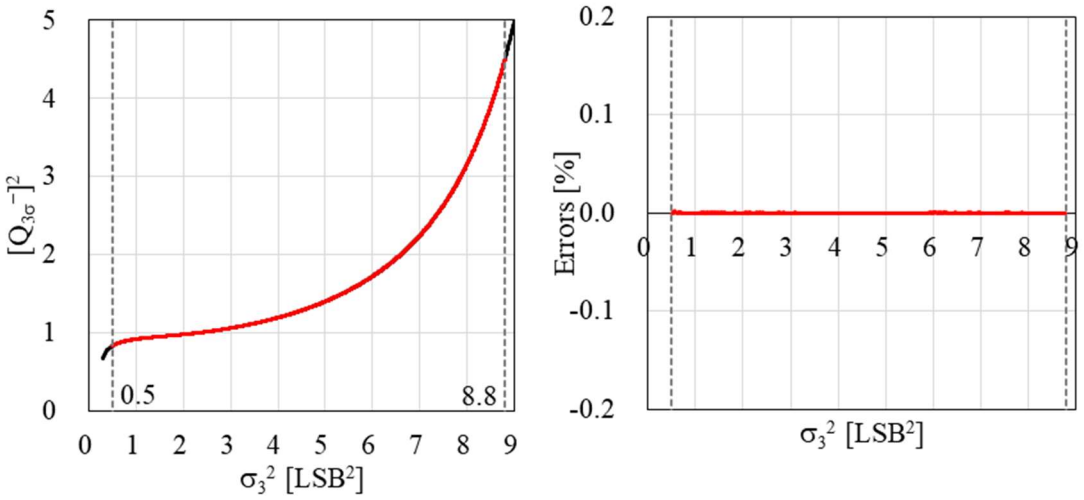

Figure 12. Computationally calculated $[Q_{3\sigma}^{-}]^2$ function and interpolated $[Q_{3\sigma}^{-}]^2$ function with a cubic spline function

(Left) Black and red lines are the calculated and interpolated $[Q_{3\sigma}^{-}]^2$ functions, respectively. The interpolation range ($0.5 \leq \sigma_3^2 \leq 8.8$) is shown by two dotted lines. (Right) Their differences are plotted by a red line on a percentage scale.

Table 12. Computationally calculated $[Q_{3\sigma}^{-}]^2$

See the "ACAC (Q3s-_T)" sheet of the "alma_memo629-tables.xlsx" Excel file.

Table 13. Coefficients of the cubic spline function for $[Q_{3\sigma}^{-}]^2$

See the "ACAC (Q3s-_T)" sheet of the "alma_memo629-tables.xlsx" Excel file.

Another cubic spline function (see Eq. (16) and Figure 13) is used to represent $Q_{3\rho}^{+}$, and the coefficients for the cubic spline function are determined as listed in Table 15 from Table 14.

$$Q_{3\rho}^{+}(x) \equiv a_i(x - x_i)^3 + b_i(x - x_i)^2 + c_i(x - x_i) + d_i \quad (16)$$
$$(\text{where } x = \sigma^2)$$

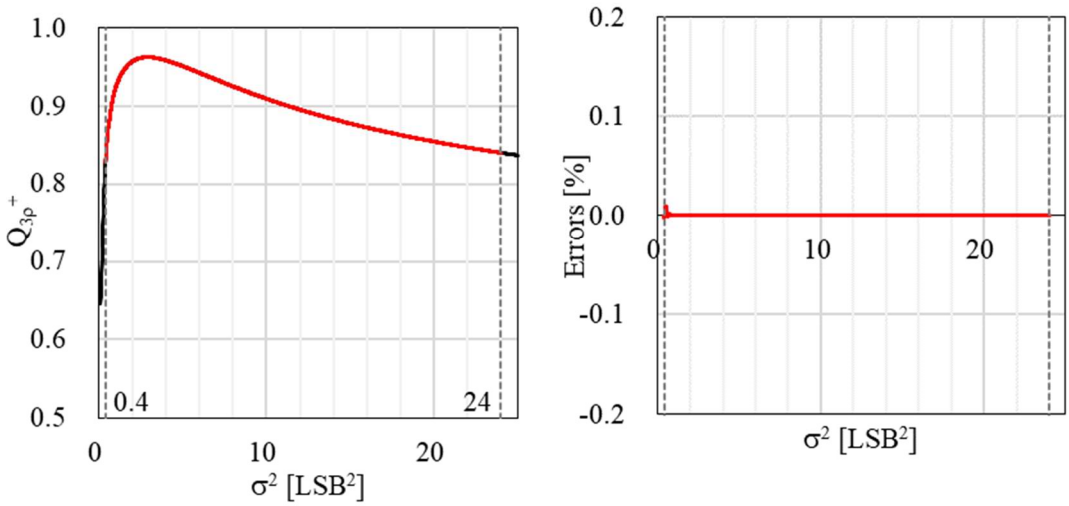

Figure 13. Computationally calculated $Q_{3\rho}^{+}$ function and interpolated $Q_{3\rho}^{+}$ function with a cubic spline function

(Left) Black and red lines are the calculated and interpolated $Q_{3\rho}^{+}$ functions, respectively. The interpolated range $(0.4 \leq \sigma^2 \leq 24.0)$ is shown by two dotted lines. (Right) Their differences are plotted by a red line on a percentage scale.

Table 14. Computationally calculated $Q_{3\rho}^{+}$

See the "ACAC (Q3r+_T)" sheet of the "alma_memo629-tables.xlsx" Excel file.

Table 15. Coefficients of the cubic spline function for $Q_{3\rho}^{+}$

See the "ACAC (Q3r+_T)" sheet of the "alma_memo629-tables.xlsx" Excel file.